

Numerical Renormalization Group Study of Random Transverse Ising Models in One and Two Space Dimensions

Yu-Cheng LIN,¹ Naoki KAWASHIMA,² Ferenc IGLÓI^{3,4} and Heiko RIEGER^{1,5}

¹*NIC, c/o Forschungszentrum Jülich, 52425 Jülich, Germany*

²*Department of Physics, Tokyo Metropolitan University, Tokyo 192-0397, Japan*

³*Res. Inst. f. Solid State Physics & Optics, 1525 Budapest, P.O.Box 49, Hungary*

⁴*Institute for Theoretical Physics, Szeged University, 6720 Szeged, Hungary*

⁵*FB 10.1 Theoret. Physik, Universität d. Saarlandes, 66041 Saarbrücken, Germany*

(Received October 31, 1999)

The quantum critical behavior and the Griffiths-McCoy singularities of random quantum Ising ferromagnets are studied by applying a numerical implementation of the Ma-Dasgupta-Hu renormalization group scheme. We check the procedure for the analytically tractable one-dimensional case and apply our code to the quasi-one-dimensional double chain. For the latter we obtain identical critical exponents as for the simple chain implying the same universality class. Then we apply the method to the two-dimensional case for which we get estimates for the exponents that are compatible with a recent study in the same spirit.

§1. Introduction

The effect of quenched randomness on disordered quantum magnets close to a quantum phase transition is much stronger than on classical systems at temperature driven phase transitions. As first observed by McCoy¹⁾ in a somewhat disguised version of a random transverse Ising chain, non-conventional scaling and off-critical singularities that lead to divergent susceptibilities even away from the critical point now appear to be a generic scenario in any dimension, at least in disordered quantum magnets with an Ising symmetry. The reason for this, as pointed out by Fisher²⁾ only recently, is a novel fixed point behavior of these systems under renormalization, namely one which is totally determined by the randomness and its geometric properties: the so-called *infinite randomness fixed point*.^{2),3)}

Within this scenario the quantum critical behavior of disordered transverse Ising models is essentially determined by strongly coupled clusters and their geometric properties.^{2),3)} Let L be the linear size of such a cluster. Then it contributes to the low energy spectrum with an exponentially small excitation gap of size $\ln \Delta E \sim L^{-\psi}$, defining the exponent ψ . Moreover, at the critical point, it has a total magnetization of size $\mu \sim L^{\phi\psi}$ defining the exponent ϕ . Finally the linear length scale of strongly coupled clusters occurring at a distance δ away from the critical point is $\xi \sim |\delta|^{-\nu}$ giving rise to a third scaling exponent ν . All bulk exponents can now be expressed via ψ , ϕ and ν , c.f. $\beta_b/\nu = x_b = d - \phi\psi$, $\nu_{\text{typ}} = \nu(1 - \psi)$ and in the Griffiths phase $z' \propto \delta^{-\nu\psi}$. For the 1d case, as treated above, it is $\psi = 1/2$, $\phi = (\sqrt{5} + 1)/2$ and $\nu = 2$ for uncorrelated disorder.

The basic geometric objects, the strongly coupled clusters, still have to be defined and this will be done within a renormalization group scheme. However, for

site or bond *dilution* it is immediately obvious what these clusters are: simply the connected clusters. Hence the critical exponents defined above are directly related to the classical percolation exponents:⁴⁾ Let $\delta = p - p_c$ be the distance from the percolation threshold, ν_{perc} the exponent for the typical cluster size, D_{perc} the fractal dimension of the percolating cluster, β_{perc} the exponent for the probability to belong to the percolating cluster. Then one has for the critical exponents defined above

$$\nu = \nu_{\text{perc}}, \quad \psi = D_{\text{perc}}, \quad \phi = (d - \beta_{\text{perc}}/\nu_{\text{perc}})/D_{\text{perc}}. \quad (1)$$

Next we consider the question, what happens for generic disorder (i.e. no dilution, but random bonds and/or fields) and we consider the model defined by the Hamiltonian

$$H = - \sum_{\langle i,j \rangle} J_{ij} \sigma_i^z \sigma_j^z - \sum_i h_i \sigma_i^x. \quad (2)$$

Here the $\{\sigma_i^\alpha\}$ are Pauli spin matrices, and the nearest neighbor interactions J_{ij} and transverse fields h_i are both independent random variables distributed uniformly:

$$\pi(J_{ij}) = \begin{cases} 1, & \text{for } 0 < J_{ij} < 1, \\ 0, & \text{otherwise,} \end{cases}$$

$$\rho(h_i) = \begin{cases} h_0^{-1}, & \text{for } 0 < h_i < h_0, \\ 0, & \text{otherwise,} \end{cases}$$

For this case the distance δ from the critical point is conveniently given by $\delta = \frac{1}{2} \ln h_0$. In one space dimension this model has been investigated intensively over the recent years,^{6), 5), 7) - 9)} and many analytical as well as numerical tools are at hand to analyze it. Beyond the simple one-dimensional geometry one has to rely on numerical techniques like quantum Monte-Carlo simulations (as in the two-dimensional case¹⁰⁾) or the numerical implementation of the renormalization group scheme, which we outline in the next section.

§2. The renormalization-group scheme

The strategy of the renormalization-group à la Ma, Dasgupta and Hu¹¹⁾ is to decrease the number of degrees of freedom and reduce the energy scale by performing successive decimation transformation in which the largest element of the set of random variables $\{h_i, J_{ij}\}$ at each energy scale is eliminated and weaker effective couplings are generated by perturbation theory.

The renormalization-group procedure is as follows: Find the strongest coupling

$$\Omega \equiv \max\{J_{ij}, h_i\}$$

in the system. If $\Omega = J_{ij}$, then the neighboring transverse fields h_i and h_j can be treated as a perturbation to the term $-J_{ij} \sigma_i^z \sigma_j^z$ in the Hamiltonian (2). The two spins involved are joined together into a spin cluster with an effective transverse field

$$\tilde{h}_{(ij)} \approx \frac{h_i h_j}{J_{ij}}$$

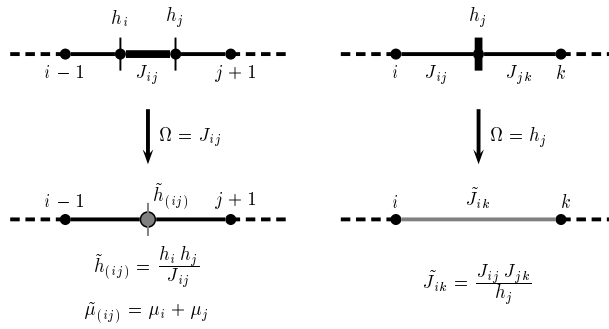


Fig. 1. Schematic of renormalization-group decimation for spin chains.

and an effective magnetic moment

$$\tilde{\mu}_{(ij)} = \mu_i + \mu_j .$$

The bonds of the new cluster $\tilde{\sigma}_{(ij)}$ with other clusters σ_k are

$$\tilde{J}_{(ij)k} \approx \max(J_{ik}, J_{jk}) .$$

If instead $\Omega = h_j$, then the associated spin σ_j is eliminated and effective bonds between each pair of its neighboring spins are generated by second-order perturbation theory. The strength of the effective bonds for each pair (i, k) is

$$\tilde{J}_{ik} \approx \max \left(J_{ik}, \frac{J_{ij} J_{jk}}{h_j} \right),$$

where the J_{ik} are the bonds that may have already been present. This procedure is sketched for the 1d case in Fig. 1. We continue the procedure until there is only one remaining spin cluster.

At each stage of the RG, an effective field (bond) is a ratio of a product of some number f of original fields (bonds) to a product of original $f - 1$ bonds (fields). The f grows under renormalization at criticality. As a result, the log-field and log-bond distributions $R_\Omega(\ln \tilde{h})$ and $P_\Omega(\ln \tilde{J})$ become broader and broader under renormalization as the critical point is approached. This increasing width of the field and bond distributions reduces the errors made by the second-order perturbation approximation. The RG becomes thereby asymptotically exact.

§3. The one-dimensional case

The RG can be carried out analytically in one space dimension,⁶⁾ therefore we can use the 1d case with periodic boundary conditions as a simple check for our numerical implementation. In Fig. 3 we show the probability distribution of the logarithm of the last remaining cluster field at the critical point $h_0 = 1$, which scales, according to Fig. 2, like $L^{-1/2}$, where L is the system size. From this one concludes that the exponent ψ defined in the introduction, is given by $\psi = 1/2$.

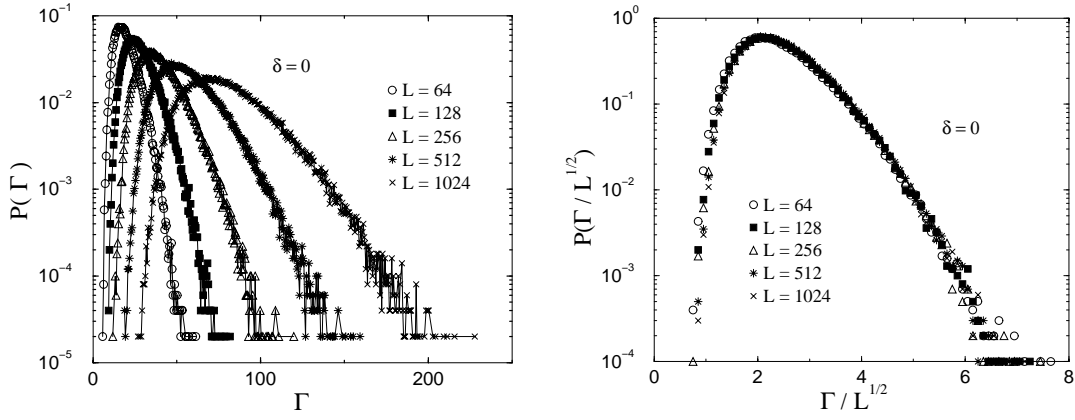


Fig. 2. **Left:** Distribution of the logarithmic strength of the last remaining cluster fields, $\Gamma \equiv \ln(\frac{\Omega_0}{\Omega_h})$ (Ω_0 denotes the energy scale of the original Hamiltonian). The distribution gets broader on a logarithmic scale with increasing system size, indicating an infinite dynamical exponent z . The data is obtained from 100 000 samples for each system size. **Right:** Scaling of the data in the left figure, assuming the exponential scaling form obtained from the analytical work.⁶⁾

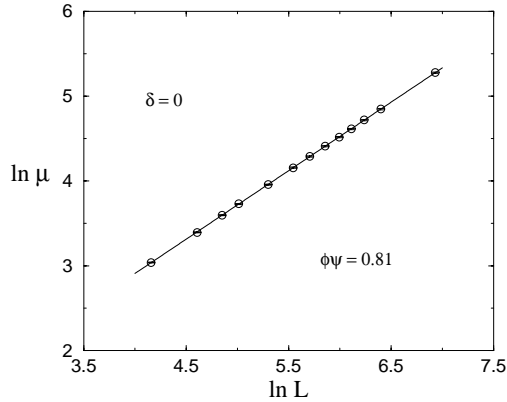


Fig. 3. Scaling of the number of active spins (proportional to average magnetic moment per spin, μ) in the last remaining spin cluster at the critical point. We find $\mu \sim L^{0.81}$ implying $\phi \approx 1.62$.

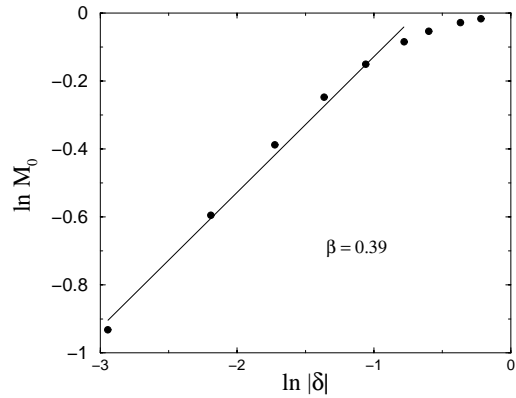


Fig. 4. In the ordered phase ($\delta < 0$), the spontaneous magnetization scales as $M_0 = |\delta|^\beta$ with $\beta \approx 0.39$. This numerical estimate of β is in agreement with the analytical prediction: $\beta = \frac{3-\sqrt{5}}{2}$. Our data is obtained by averaging over 100 000 samples of size $L = 1024$.

Inspecting the number of active spins in the last remaining cluster at the critical point we obtain the size dependence $\mu \sim L^{0.81}$ from Fig. 3, and thus $\phi \approx 1.62$.

In the Griffiths phase $h_0 \neq 1$, the probability distribution of the energy gap Ω still has an algebraic singularity at $\Omega = 0$, and its finite size scaling behavior is

$$\Omega P_L(\Omega) \propto L^d \Omega^{d/z'(\delta)} = (L^{z'(\delta)} \Omega)^{d/z'(\delta)}, \quad (3)$$

where d is the space dimension (in this section $d = 1$) and $z'(\delta)$ a generalized dynamical exponent that varies continuously with the distance δ from the critical point.

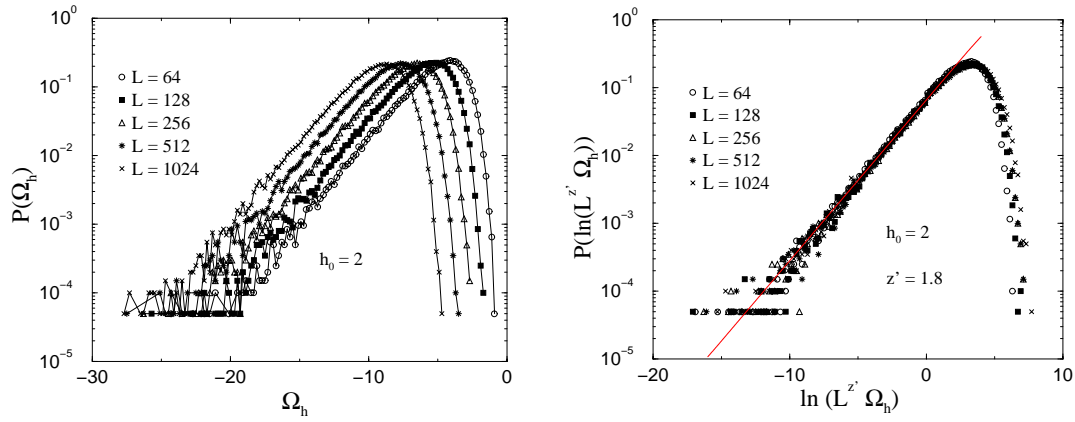


Fig. 5. **Left:** Distribution of logarithmic effective fields Ω_h of the last spin cluster in the disordered phase at $h_0 = 2$. The curves for different sizes look very similar but shifted horizontally related to each other. **Right:** Scaling plot of the data in the left figure. The typical fields and spacing of rare large strongly coupled clusters in the disordered phase is related via $\Omega \sim L^{z'}$. The dynamical exponent $z'(h)$ is obtained from the asymptotic form $\ln P(\ln \Omega_h) = 1/z'(h)(\ln \Omega_h) + \text{const.}$ ⁵⁾

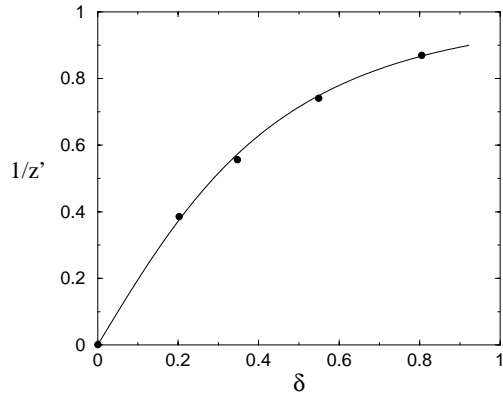


Fig. 6. The value of $1/z'(\delta)$ for $d = 1$ obtained from the probability distribution of logarithmic effective fields of the last remaining clusters in the Griffiths-McCoy region. The solid line, which fits well, is a plot of the exact $z'(\delta)$ -relation reported in Ref.⁸⁾: $z' \log(1 - z'^{-2}) = -2h_0$.

This exponent parameterizes the strength of all singularities in the off-critical region $\delta \neq 0$, for instance in the disordered phase $\delta > 0$ one has for the imaginary time autocorrelations $G_{\text{loc}}(\tau) = [\langle \sigma_i^x(\tau) \sigma_i(0) \rangle_{T=0}]_{\text{av}} \sim \tau^{-1/z'(\delta)}$, for the local susceptibility $\chi_{\text{loc}} \sim T^{1/z'(\delta)-1}$, for the specific heat $C \sim T^{1/z'(\delta)}$ and for the magnetization in a longitudinal field $M \sim H^{1/z'(\delta)}$. The most convenient way to determine this exponent is, however, via the distribution $P_L(\Omega)$. At the critical point this distribution has to merge with the critical distribution discussed above — and therefore $\lim_{\delta \rightarrow 0} z'(\delta) = \infty$. Using this finite-size scaling form for the distribution of the last bonds/fields in the RG procedure we can extract the dynamical exponent as is done in Fig. 5.

In the ordered phase $h_0 < 1$ the distribution of fields and bonds are related to the distribution in the disordered phase $h_0 > 1$ via duality, see Fig. 7.

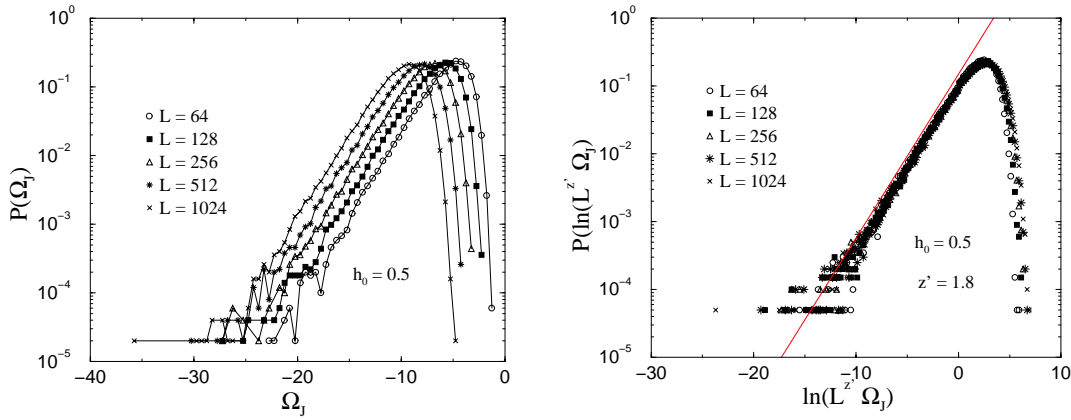


Fig. 7. Distribution of last log-bonds (left) in the ordered phase at $h_0 = 0.5$ for $d = 1$ and its scaling plot (right). One observes that the scaling behavior of bonds in the ordered phase and that of fields in the disordered phase (see Fig. 5) are related through duality.

§4. The double chain

The RG scheme for double chains with some new elements (compared to the 1d case treated above) is depicted in Fig. 8.

As in 1d, we observe that the log-field and log-bond distributions get broader with increasing system size at criticality. To estimate the critical point we compute the field distribution at the last stage of the RG varying the initial transverse field h_0 . We estimate the critical point to be at $h_0 = 1.9$, beyond which the broadening of the log-field distribution appears to be saturating, as for 1d in the Griffiths phase. Moreover at $h_c = 1.9$ the log-field and the log-bond distributions become asymptotically identical except for a constant multiplicative factor that reflects the short-ranged non-universal physics (see Fig. 9). This is obvious in the single chain, where it follows from the self-duality of the simple chain at the critical point. However, the double chain is *not* self-dual, nevertheless the scaling forms of the two distributions become identical at the critical point. We speculate that this remains true also in the two-dimensional case to be discussed below.

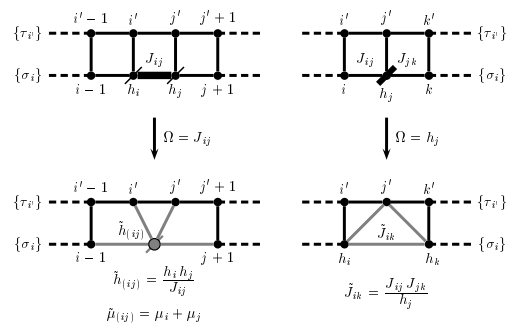


Fig. 8. Schematic of renormalization-group decimation for double chains used in the numerical simulations.

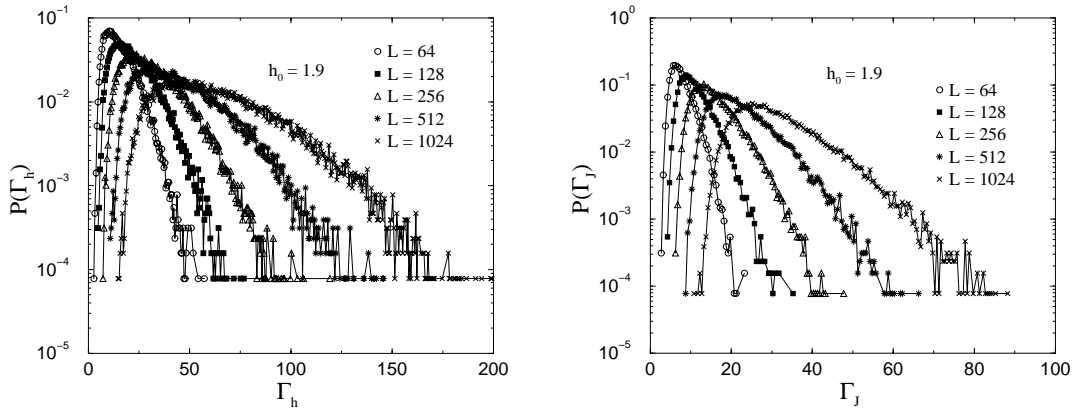


Fig. 9. The log-field (left) and log-bond (right) distribution for the double-chain at $h_c = 1.9$. The data is obtained from 25 600 samples for each system size.

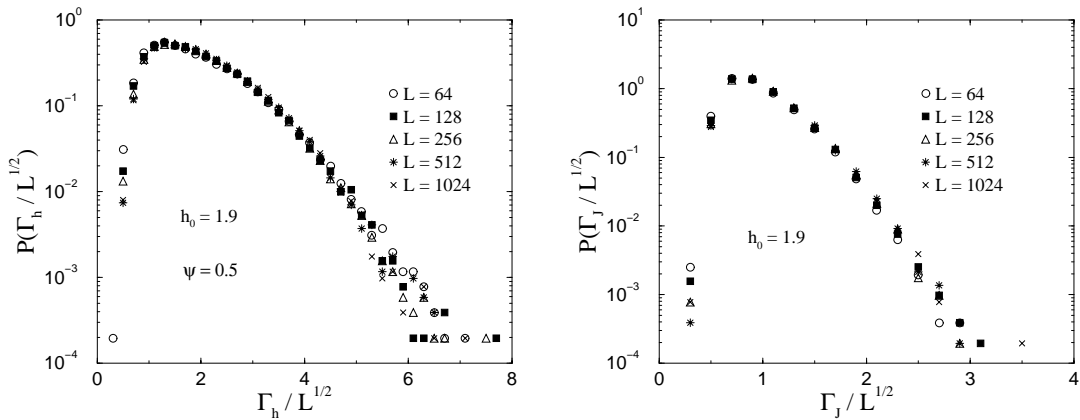


Fig. 10. Scaling plots of the distribution of log-fields (left) and of log-bonds (right) for the double-chain at the critical point ($h_c = 1.9$). The data scales quite well with the same form $\Gamma_{h(J)} \equiv \ln\left(\frac{\Omega_0}{\Omega_{h(J)}}\right) \sim \sqrt{L}$ as in 1d.

The scaling of the critical distributions depicted in Fig. 9 yields the critical exponent $\psi = 0.5$, as shown in Fig. 10. This is the same as for the simple chain. In addition, for the average magnetic moment of the last remaining cluster at $h_c = 1.9$, we find the same system size dependence for the double chain as for the 1d case, i.e. the same critical exponent ϕ , see Fig. 11. This implies that the double chain and the simple chain belong to the same universality class.

In the Griffiths phase $h_0 > h_c = 1.9$ we extracted the generalized exponent $z'(h_0)$, which is depicted in Fig. 12. Close to the critical point h_c we observe the same linear dependence of $1/z'(\delta)$ on the distance $\delta = h_0 - h_c$ from the critical point as in 1d. Since for $\delta \ll 1$ one expects $z'(h_0) \propto \delta^{-\psi\nu}$ this implies that $\nu = 2$ the same as the simple chain.

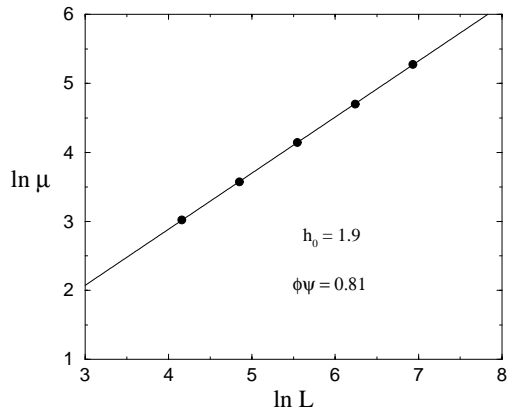


Fig. 11. A log-log scaling plot of the average magnetic moment per cluster, μ , with the linear system size L at the estimated critical point $h_c = 1.9$ for the double chain. We find the same exponent ϕ as in 1d.

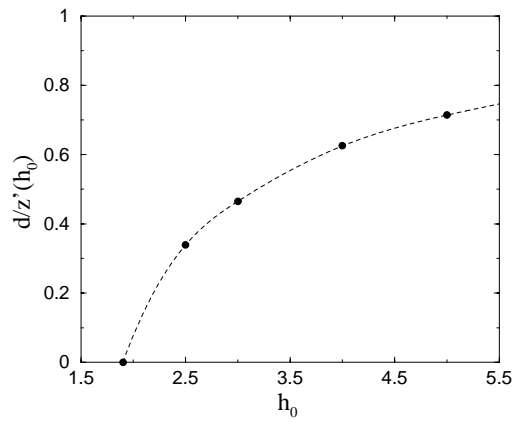


Fig. 12. Estimates for $1/z'$ against h_0 for the double chain.

§5. The square lattice (2d)

Next we present our preliminary results for the two-dimensional (2d) case with periodic boundary conditions, where we, in contrast to the treatment in Motrunich et al.,³⁾ keep *all* bonds generated during renormalization. The RG scheme for the 2d case is very similar to the one for the double chain and is depicted in Fig. 13.

In comparison to 1d and the double chain models, the location of the critical point cannot be fixed precisely for two dimensions according to our numerical obser-

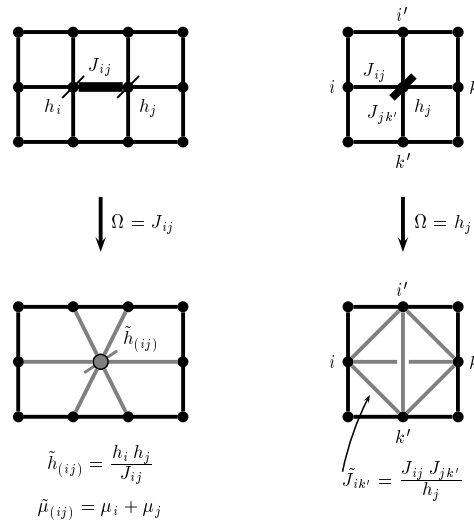


Fig. 13. Renormalization-group decimations for the two-dimensional (square) lattice used in the numerical simulations.

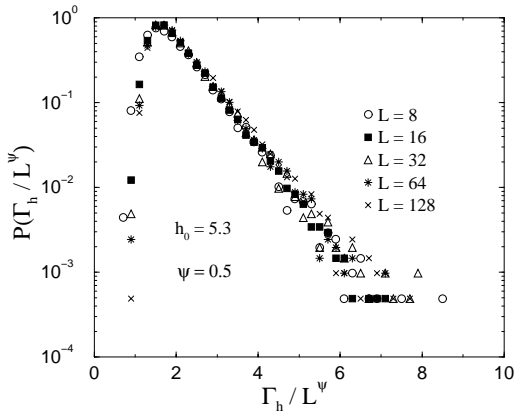


Fig. 14. Scaling of the log-fields for $d = 2$ at the last stage of the RG at what we estimate to be the critical point.

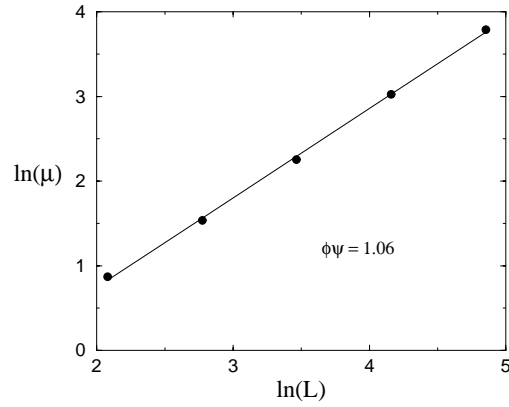


Fig. 15. A scaling plot of the number of the active spins in the last remaining cluster at our candidate critical point $h_0 = 5.3$.

vation so far. We obtain a critical field approximately at $h_0 = 5.3$ by applying the criterion that field and bond distribution should have the similar scaling form (as for the 1d case and the double chain). The scaling of the last log-field distribution yields $\psi \approx 0.5$ and the scaling plot of the number of the active spins in the last remaining cluster yields $\phi \approx 2.0$ and $\mu \sim L^{1.06}$.

Our preliminary results for the two-dimensional case agree with those obtained recently by Motrunich et al.³⁾ and with those obtained by us via quantum Monte-Carlo simulation.¹⁰⁾

Acknowledgments

H. R. is grateful to the German research foundation (DFG) for financial support within a JSPS-DFG binational (Japan-Germany) cooperation. N. K.'s works is supported by a Grant-in-Aid for Scientific Research Program (No.11740232) from Mombusho, Japan.

References

- 1) B. M. McCoy, Phys. Rev. Lett. **23** (1969), 383.
- 2) D. S. Fisher, Physica **A263** (1999), 222.
- 3) O. Motrunich, S.-C. Mau, D. A. Huse and D. S. Fisher, cond-mat/9906322.
- 4) T. Senthil and S. Sachdev, Phys. Rev. Lett. **77** (1996), 5292.
- 5) A. P. Young and H. Rieger, Phys. Rev. **B53** (1996), 8486.
- 6) D. S. Fisher, Phys. Rev. Lett. **69** (1992), 534; Phys. Rev. **B51** (1995), 6411.
- 7) F. Iglói and H. Rieger, Phys. Rev. **B57** (1998), 11404.
- 8) F. Iglói and H. Rieger, Phys. Rev. **E58** (1998), 4238.
- 9) H. Rieger and F. Iglói, Phys. Rev. Lett. **83** (1999), 3741.
F. Iglói, R. Juhász and H. Rieger, Phys. Rev. **B59** (1999), 11308.
F. Iglói, D. Karevski and H. Rieger, Europ. Phys. J. **B5** (1998), 613.
H. Rieger and F. Iglói, Europhys. Lett. **39** (1997), 135.
F. Iglói and H. Rieger, Phys. Rev. Lett. **78** (1997), 2473.
- 10) C. Pich, A. P. Young, H. Rieger and N. Kawashima, Phys. Rev. Lett. **81** (1998), 5916.
H. Rieger and N. Kawashima, Europ. Phys. J. **B9** (1999), 233.

- T. Ikegami, S. Miyashita and H. Rieger, *J. Phys. Soc. Jpn.* **67** (1998), 2761.
- 11) S. K. Ma, C. Dasgupta and C.-K. Hu, *Phys. Rev. Lett.* **43** (1979), 1434.
C. Dasgupta and S. K. Ma, *Phys. Rev.* **B22** (1980), 1305.